CHILEAN JOURNAL of AGRICULTURAL RESEARCH
RESEARCH ARTICLE

Antifungal efficacy of *Aloe vera*-mediated silver nanoparticles in different concentrations and application methods against *Fusarium oxysporum* in *Cucurbita pepo*

Eman Selim[1*], Esraa Saeed[1], Yasser Selem[2], Mayasar I. Al-zaban[3], Eman Fayad[4], Asim Ahmed S. Alsenani[4], Hana Alsufyani[4], and Hanan Abdallah[1*]

[1]Zagazig University, Faculty of Science, Plant Physiology Department, Zagazig 44511, Egypt.
[2]Zagazig University, Faculty of Specific Education, Organic Chemistry Department, Zagazig 44511, Egypt.
[3]Princess Nourah bint Abdulrahman University, College of Science, Department of Biology, Riyadh 11671, Saudi Arabia.
[4]Taif University, College of Sciences, Department of Biotechnology, Taif 21944, Saudi Arabia.
[*]Corresponding author (eman8_extra8@yahoo.com; h.abdallah@zu.edu.eg)
Received: 21 December 2025; Accepted: 8 April 2026, doi:10.4067/S0718-58392026000400545

ABSTRACT

Fusarium wilt seriously threatens *Cucurbita pepo* L. production worldwide. Plant-based nanotechnology antifungals offer a promising and eco-friendly control strategy. This study investigated the antifungal efficacy of *Aloe vera* (L.) Burm. f.-mediated Ag nanoparticles (Ag-NPs) against *Fusarium oxysporum*. Biogenic Ag-NPs were synthesized using *A. vera* leaf extract with an average crystallite size of 15.22 nm and a surface plasmon resonance peak at 413 nm. In vitro, Ag-NPs at 2.5, 5, 10, and 15 mg L^{-1} generated dose-dependent inhibition zones (0.5-2.0 cm). The concentration 15 mg L^{-1} produced the largest inhibition zone (2.0 cm) and the greatest reduction in colony diameter. In vivo greenhouse trial, Ag-NPs were tested at 2.5, 5, 10, and 15 mg L^{-1} by foliar spray or soil drench (pre-planting) on *Fusarium*-inoculated plants *vs*. uninoculated and inoculated controls. *Fusarium* infection severely reduced plant growth (47%-155%), photosynthetic pigments (47%-58%), and mineral elements (30%-80%) compared to the uninoculated control (T1). However, Ag-NPs applications displayed strong antifungal agents and plant biostimulants. In particular, 15 mg L^{-1} foliar Ag-NPs (T5) displayed the significant improvement in leaf number (43.1%), shoot length (42.9%), biomass (68.0%-154.5%), chlorophyll *a* and *b* (112.5% and 100%), phenols (40.0%), sugars (14%), and minerals Ca/Mg/Na/K (42.9%, 150.0%, 150.0%, and 42.9%) compared to the inoculated control. Moreover, increasing Ag-NPs concentration mitigated oxidative stress in infected plants by enhancing activities of catalase, superoxide dismutase, polyphenol oxidase, and peroxidase. Multivariate analyses (principal component analysis and heatmap) showed that high-dose Ag-NPs were associated with improved growth and mineral traits, antioxidant and osmoprotective metabolites.

Key words: Antifungal activity, antioxidant enzymes, cucurbit wilt, green synthesis, phytochemicals, silver nanoparticles.

INTRODUCTION

Cucurbita pepo L. is an important crop in vegetable production systems (Magalhães et al., 2025). It is valued for its nutritional content and economic significance. It is highly susceptible to Fusarium wilt, which threatens its cultivation (Grumet et al., 2021). Fusarium wilt is caused by soil-borne fungus *Fusarium oxysporum* (Gilardi et al., 2024). This pathogen causes wilting, stunting, and eventual plant death (Choi et al., 2015). The high economic losses of this fungus require effective and sustainable management strategies. Conventional methods of controlling *Fusarium* rely on synthetic fungicides. Long-term utilization of these chemicals poses

significant environmental and leave toxic residues health risks (Macías Sánchez et al., 2023). This has prompted shift towards eco-friendly and sustainable alternatives for plant disease control.

Nanotechnology offers promising solution by utilizing nanoparticles (NPs). Nanoparticles possess unique physical and chemical properties due to their small size (Joudeh and Linke, 2022). Silver nanoparticles (Ag-NPs) are a powerful antimicrobial agent due to their high reactivity and large surface area. Moreover, Ag-NPs disrupt multiple cellular targets in phytopathogens (Qureshi et al., 2023). However, physical methods of nanoparticle production are often energy-intensive and rely on toxic reagents. This limits their suitability for sustainable agriculture. Otherwise, green synthesis using plant extracts offers an attractive alternative. Studies have recently demonstrated the effectiveness of green-synthesized Ag-NPs against plant pathogens (Usman et al., 2024). The mechanism of action disrupts the fungal cell wall, inhibits essential enzymes, and causes cell death (Gonzalez-Jimenez et al., 2023).

The application of nanotechnology and bioactive derivatives has emerged as a critical strategy for enhancing crop resilience against both abiotic and biotic stressors in modern agriculture. Research has demonstrated that nanoparticle-based biostimulants are highly effective in mitigating environmental pressures, such as drought tolerance in potato crops (Alowaiesh et al., 2024) and alleviating the detrimental morphological and molecular effects of salinity stress (Alahmari et al., 2025). Furthermore, specialized nano-priming techniques, such as the use of calcium silicate nanoparticles ($CaSiO_3$NPs), have been shown to significantly promote germination, seedling growth, and antioxidant enzyme activity in rice genotypes under water-deficit conditions (Alwan et al., 2026). Beyond abiotic stress, the integration of organic derivatives, such as black soldier fly frass, provides a sustainable biofungicidal approach to managing devastating soil-borne pathogens like *Fusarium* wilt in bananas (Ong et al., 2025). Together, these advancements highlight a multi-faceted approach to stabilizing crop yields and improving plant health through innovative physiological and molecular interventions.

Recently, researchers have focused on green synthesis using biological and non-toxic alternatives (Arsène et al., 2023). *Aloe vera* (L.) Burm. f. is an ideal candidate for this process (Arsène et al., 2023). Its leaves are rich in bioactive compounds such as polysaccharides, flavonoids, and saponins (Burange et al., 2021). This biogenic approach is not only eco-friendly but also cost-effective and safe (Macías Sánchez et al., 2023). *Aloe vera*-mediated AgNPs have shown significant antifungal activity against fungi (Arsène et al., 2023). Therefore, this study aimed to evaluate the antifungal efficacy of *A. vera*-mediated Ag-NPs against *Fusarium oxysporum*. This was performed through in vitro inhibition assays and in vivo greenhouse trials on *C. pepo*. Specifically, their impact on mycelial growth suppression, plant growth restoration, physiological recovery, and antioxidant enzyme modulation were assessed under Fusarium wilt stress. These findings could establish the potential of green-synthesized Ag-NPs as an eco-friendly alternative for sustainable Fusarium wilt management.

MATERIALS AND METHODS

This study used silver nitrate ($AgNO_3$) for the synthesis of nanoparticles. Extract from *Aloe vera* (L.) Burm. f. leaves was utilized as a capping agent. All of the analytical-grade reagents used were acquired from Sigma-Aldrich, St. Louis, Missouri, USA.

Extraction and preparation of *A. vera* leaf gel

Fresh and healthy *A. vera* leaves were collected from the Horticulture Department, Faculty of Agriculture, Zagazig University, Egypt. The leaves were washed with tap water and then sterile distilled water. After carefully removing the outer skin, the inner gel was blended into a homogeneous mixture. The homogenate was filtered using Whatman N°1 filter paper. The clear extract was stored at -4 °C until further use (Abdalla et al., 2022).

Alkaloids, flavonoids, steroids, and saponins were screened in the extract using standard phytochemical procedures according to Iqbal et al. (2015). Characterization of phenolic compounds was performed with high-performance liquid chromatography (HPLC). The compounds were identified by comparing their retention times with authentic standards according to Wu et al. (2013).

Biosynthesis and characterization of Ag nanoparticles

The synthesis of Ag nanoparticles (Ag-NPs) was applied by combining 20 mL *A. vera* extract with 20 mL 0.3 M $AgNO_3$ solution. The mixture was stirred continuously at room temperature for 30 min. Following this, the

reaction mixture was heated in a 100 mL Teflon-lined container (Parr Instrument Company, Moline, Illinois, USA) under carefully controlled temperature and time conditions. The precipitate after natural cooling was filtered and washed with diH_2O. The final product was dried at 60 °C for 6 h. The properties of synthesized Ag-NPs were measured between 200 and 500 nm using a UV-Vis spectrophotometer (Ultra-3660, Rigol Technologies, Beijing, China). Fourier transform infrared (FTIR) spectroscopy was employed to identify the functional groups that stabilized the nanoparticles. The X-ray diffraction was used to obtain crystallographic patterns at 2θ values ranging from 30° to 140° with a Cu Kα1 X-ray diffractometer. Finally, the size and shape of the Ag-NPs were determined by high-resolution transmission electron microscopy (HR-TEM) at the National Research Centre in Cairo, Egypt. For this analysis, the nanoparticles were suspended in ethanol, sonicated, and then drop-cast onto copper grids for examination with a JEM2100 HR-TEM (JEOL, Tokyo, Japan).

In vitro antifungal assay

Agar well diffusion method was utilized to assess the antifungal activity of synthesized Ag-NPs against *Fusarium oxysporum*. Potato dextrose agar (PDA) plates were inoculated with fungal spores. These plates were supplemented with Ag-NPs at concentrations of 2.5, 5, 10, and 15 mg L^{-1}. Then plates were incubated in the dark for 7 d at 25 °C. Fungal growth inhibition was determined by measuring the diameter of the fungal colonies. The inhibition of *F. oxysporum* mycelial growth was evaluated using a modified agar diffusion technique. A stock solution of Ag-NPs was incorporated into autoclave-sterilized PDA to achieve final concentrations of 2.5, 5, 10, and 15 mg L^{-1}. Fungal spores were suspended in 20 mL distilled water from pre-grown agar plates. A 100 µL volume of the spore solution was used to inoculate fresh PDA plates. They were then spread with a sterile L-shaped plastic spreader. These new plates were incubated for 72 h at 25 °C in the dark. Subsequently, a sterile cork borer (8 mm in diameter) was used to transfer a plug from the pre-grown plates to the center of each new, Ag-NP-treated PDA plate. The plates were then incubated in the dark at 25 °C for 7 d. The diameter of the fungal colonies was recorded in millimeters after the incubation period (Akpinar et al., 2021).

In vivo greenhouse experiment

The efficacy of Ag-NPs in enhancing the resistance of *Cucurbita pepo* L. to Fusarium wilt disease was assessed under greenhouse conditions. Sterilized pots measuring 60 cm by 15 cm were filled with steam-sterilized sand-clay soil (1.5 kg per pot). One week before planting, pots were inoculated with 50 mL *F. oxysporum* inoculum. The soil moisture was maintained. The inoculum had a spore count of 5×10^8 spores mL^{-1}. The pots were arranged in a completely randomized design with six replicates. The experiment included the following five treatments. The control (T1) consisted of seeds planted in sterilized soil without inoculation; T2 involved planting seeds in soil inoculated with *F. oxysporum*; T3 was planted with seeds in sterilized soil, then seedlings were treated with a foliar spray of Ag-NPs at concentrations of 2.5, 5, 10, and 15 mg L^{-1}. The foliar application was applied after 5 and 20 d. In T4, seeds were planted in soil pre-treated with Ag-NPs at the same four concentrations. Finally, T5 contained seeds planted in inoculated soil, and seedlings received a foliar spray of Ag-NPs at the same concentrations and time as T3. Four weeks after the application of AgNPs, seedlings were collected to measure the shoot length (cm), number of leaves, and shoot fresh and dry weight (g). For each replicate, three seedlings were randomly selected. In addition, fresh leaf samples were randomly collected from each treatment in the early morning to analyze photosynthetic pigment content. Specifically, 100 mg fresh leaves were homogenized in 10 mL 85% acetone to extract chlorophyll *a* and *b*. The extract absorbance was measured at wavelengths of 663 and 644 nm using a UV-visible spectrophotometer (Model Ultra-3660, Rigol Technologies), with pure 85% acetone as the blank, following the method of Metzner et al. (1965). The concentrations of chlorophylls (*a*, *b*) were then calculated in µg mL^{-1} using the appropriate formulas, taking the dilution factor into account. To measure the total phenolic content, we extracted a 0.5 g sample of *C. pepo* leaves. It was quantified spectrophotometrically using the Folin-Ciocalteu reagent (Jindal and Singh, 1975). Total soluble sugars were quantified spectrophotometrically at 625 nm according to Prud'homme et al. (1992). Proline content was determined spectrophotometrically at 520 nm using a proline standard curve following Bates et al. (1973). Total protein content was determined by measuring total N using micro-Kjeldahl method (Silva et al., 2016). The total N value was multiplied by a conversion factor of 6.25. Plant mineral elements (Ca^{2+}, Mg^{2+}, Na^{+}, K^{+}) were determined following Naga Raju et al. (2006). The mineral elements were measured by digesting 0.1 g air-dried samples in concentrated HNO_3 until clear. Then diluting with distilled water and

analyzing Ca^{2+} and Mg^{2+} via atomic absorption spectrophotometer (2380, Perkin-Elmer, Waltham, Massachusetts, USA) and Na^{+} and K^{+} via flame photometer. Antioxidant enzyme activities were measured spectrophotometrically. Catalase (CAT) was measured by H_2O_2 consumption at 240 nm (Bergmeyer, 1965). Peroxidase (POD) was recorded at 470 nm following the method of Bergmeyer (1965). Superoxide dismutase (SOD) was recorded using nitro blue tetrazolium reduction (Dhindsa et al., 1981). Polyphenol oxidase (PPO) was measured by initial absorbance increase at 420 nm (Soliva et al., 2000).

Data analysis

Significant differences among different treatments for the measured traits were determined using the LSD test at a significance level of $P < 0.01$. The analyses and visualizations were performed using Statistica software, version 14.2.0. (TIBCO Software, Palo Alto, California, USA). The principal component biplot and heatmap were applied using ggplot2, factoextra, and FactoMineR in R programming (R Foundation for Statistical Computing, Vienna, Austria).

RESULTS

Phytochemical composition and Ag-NP characterization

Phytochemical screening of the aqueous *Aloe vera* extract confirmed the presence of alkaloids, flavonoids, glycosides, saponins, and steroids. Besides, HPLC identified several phenolic compounds, with kaempferol as the predominant phenolic compound. The successful synthesis of Ag-NPs was demonstrated using multiple analytical techniques (Figure 1). A clear color change from greenish-yellow to brown indicated the reduction of Ag^{+} ions. The UV-Vis spectrophotometry showed a characteristic surface plasmon resonance (SPR) peak at 413 nm. Fourier-transform infrared spectroscopy (FTIR) confirmed the presence of stabilizing hydroxyl, amine, and polysaccharide groups. The X-ray diffraction analysis revealed a hexagonal crystalline structure. The calculated average crystallite size of 15.22 nm. Moreover, HR-TEM images showed that the synthesized nanoparticles were predominantly spherical with diameters ranging from 9.26 to 31.18 nm.

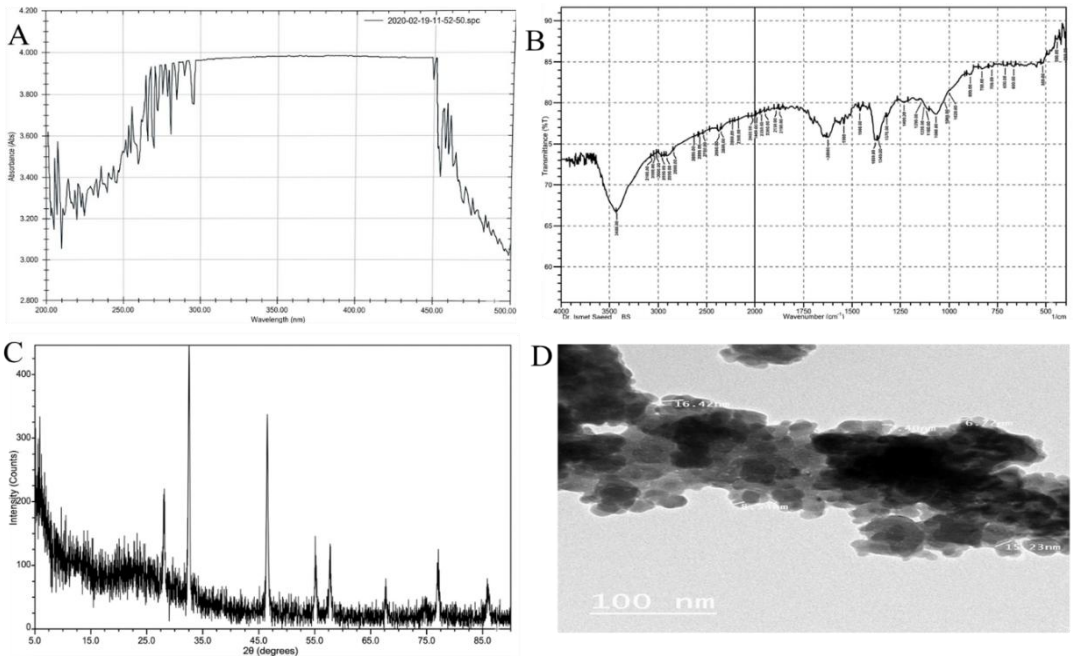

Figure 1. Characterization of biogenic Ag nanoparticles (Ag-NPs). A. UV-Vis absorption spectrum of the biogenic Ag-NPs. B. Fourier transform infrared (FTIR) spectrum of the synthesized Ag-NPs. C. X-ray diffraction (XRD) pattern of the biogenic Ag-NPs. D. High-resolution transmission electron microscopy (HR-TEM) micrograph of the biogenic Ag-NPs.

In vitro antifungal activity of biogenic Ag-NPs

All tested concentrations of biogenic Ag-NPs (2.5, 5, 10, and 15 mg L^{-1}) strongly inhibited mycelial growth of *Fusarium oxysporum* (Figure 2). The agar well diffusion assay revealed inhibition zones increasing from 0.5 cm at 2.5 mg L^{-1} to 2.0 cm at 15 mg L^{-1}. The concentration of 15 mg L^{-1} proved mycelial suppression and the largest inhibition zone (2.0 cm). The high concentration surpassed the lower doses by 300%. This fully aligns with methods using spore-inoculated PDA plugs and represents maximum *F. oxysporum* growth restriction.

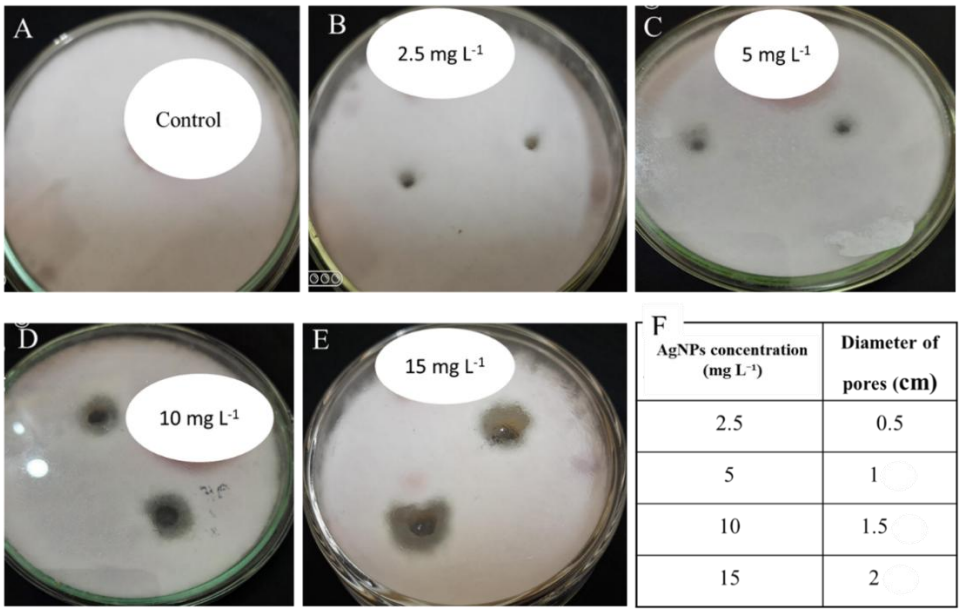

F

AgNPs concentration (mg L^{-1})	Diameter of pores (cm)
2.5	0.5
5	1
10	1.5
15	2

Figure 2. In vitro antifungal activity of biogenic Ag nanoparticles (Ag-NPs) against *Fusarium oxysporum* using agar well diffusion method at concentrations of control (A), 2.5 mg L^{-1} (B), 5 mg L^{-1} (C), 10 mg L^{-1} (D), and 15 mg L^{-1} (E); indicating the diameter of pores (cm) relative to each Ag-NPs concentration (F).

In vivo greenhouse experiment

The greenhouse experiment evaluated the impact of *A. vera*-synthesized Ag-NPs on *C. pepo* plants under Fusarium stress. All Ag-NPs treatments significantly enhanced plant growth traits compared to the uninoculated control and the pathogen-only treatment (Figure 3). The Ag-NPs treatments significantly mitigated *F. oxysporum*-induced stress in *C. pepo*. *Fusarium* inoculation (T2) reduced number of leaves by 47.22%, shoot length by 42.9%, fresh weight by 86.4%, and dry weight by 154.6% compared to the uninoculated control (T1) (Figure 4). Foliar Ag-NPs at 15 mg L^{-1} (T3) increased these traits by 75.0%, 76.1%, 200.8%, and 221.8% compared to T2 in the same order. In infected plants, T5-15 mg L^{-1} enhanced plant growth by 43.1% (leaf number), 42.9% (shoot length), 68.0% (fresh weight), and 154.5% (dry weight). The soil treatment (T4-15) enhanced plant growth by 69.4% (leaf number), 72.4% (shoot length), 167.2% (fresh weight), and 214.5% (dry weight) Pathogen stress (T2) decreased chlorophyll *a* and *b* by 47%-58% compared to T1. However, T5-15 mg L^{-1} enhanced these parameters by 112.5% and 100.0%, respectively (Table 1). Besides, T5-15 enhanced total phenols by 40.0%, soluble sugars 14.0%, proline content by 9.9% and total protein 14.8% in compared T2. The T5-15 mg L^{-1} elevated Ca by 42.9%, Mg by 150.0%, Na by 150.0%, and K by 42.9% compared to T2 (Table 2). The T3-15 mg L^{-1} boosted CAT by 275%, SOD 236%, PPO 242%, and POD 183% *vs*. T1, priming defenses (Figure 5). In infected T5-15 plants, Ag-NPs reduced pathogen-induced enzyme elevations by 35%-52%, normalizing oxidative stress responses. Infection (T2) elevated CAT, SOD, PPO, and POD activities signaling oxidative stress (Figure 4). The T3-15 mg L^{-1} peaked enzymes at CAT (7.75 units), SOD (13.6 units), PPO (6.8 units), and POD (0.61 units). The T5-15 mg L^{-1} modulated activities toward control levels while sustaining stress mitigation.

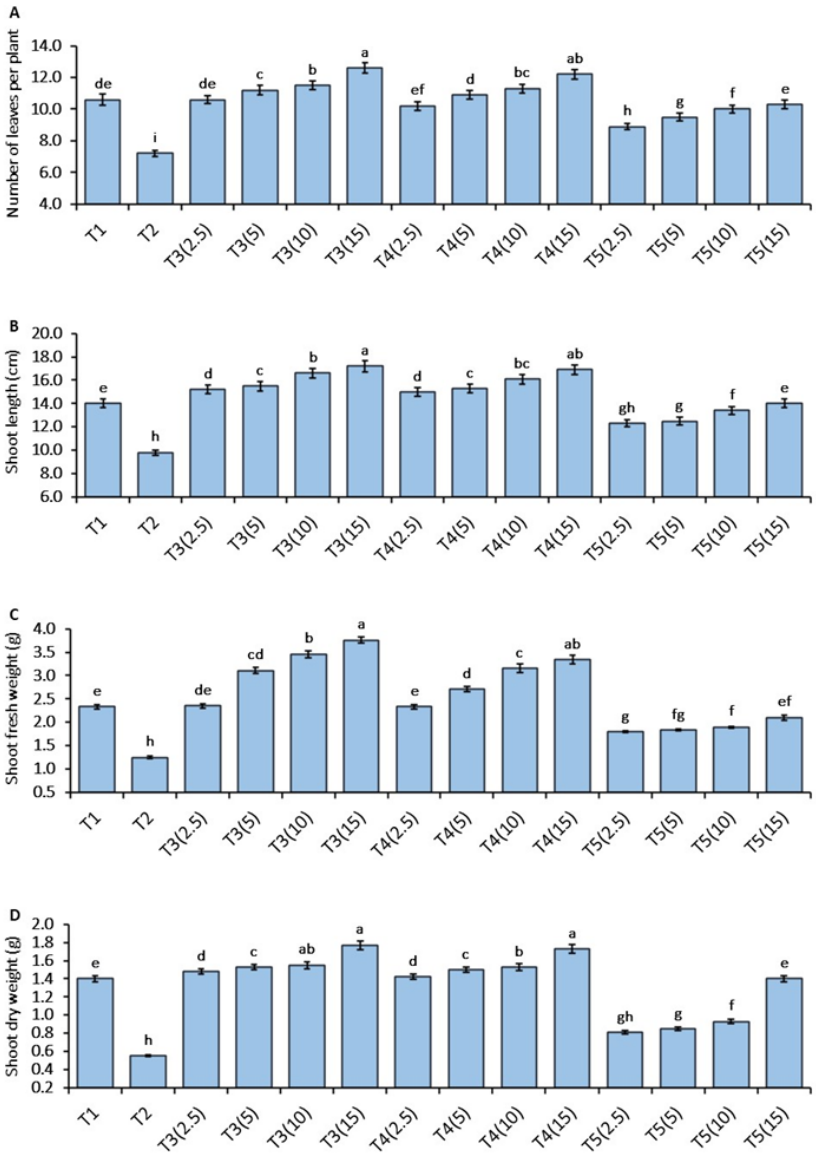

Figure 3. Effect of *Aloe vera*-synthesized Ag nanoparticles (Ag-NPs) on the number of leaves per plant (A), shoot length (B), shoot fresh weight (C), and shoot dry weight (D) of *Cucurbita pepo*. The bars on the columns are the standard deviation, and different letters indicate significant differences between means ($LSD_{0.01}$). T1: Control (sterilized soil, no inoculation); T2: pathogen (*Fusarium oxysporum* inoculated soil); T3: foliar spray of *A. vera*-synthesized Ag-NPs at 2.5, 5, 10, 15 mg L^{-1} (sterilized soil, applied days 5 and 20); T4: seeds planted in soil pre-treated with *A. vera*-synthesized Ag-NPs at 2.5, 5, 10, and 15 mg L^{-1}; T5: combined treatment with planted seeds in *Fusarium*-inoculated soil and seedlings received foliar sprays of *A. vera*-synthesized Ag-NPs at 2.5, 5, 10, and 15 mg L^{-1}.

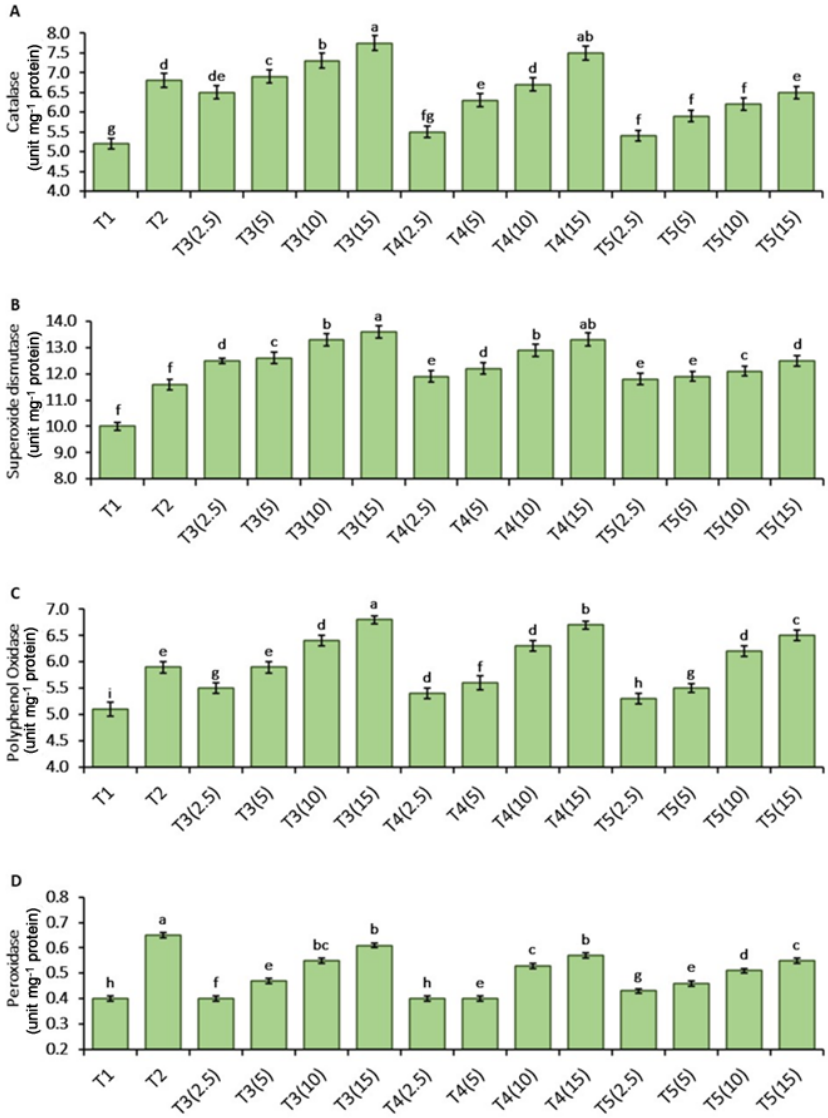

Figure 4. Effects of *Aloe vera*-synthesized Ag nanoparticles (Ag-NPs) on the catalase (A), superoxide dismutase (B), polyphenol oxidase activity (C), and peroxidase (D) enzymes of *Cucurbita pepo.* The bars on the columns are the standard deviation, and different letters indicate significant differences between means ($LSD_{0.01}$). T1: Control (sterilized soil, no inoculation); T2: pathogen (*Fusarium oxysporum* inoculated soil); T3: Foliar spray of *A. vera*-synthesized Ag-NPs at 2.5, 5, 10, 15 mg L^{-1} (sterilized soil, applied days 5 and 20); T4: seeds planted in soil pre-treated with *A. vera*-synthesized Ag-NPs at 2.5, 5, 10, and 15 mg L^{-1}; T5: combined treatment with planted seeds in *Fusarium*-inoculated soil and seedlings received foliar sprays of *A. vera*-synthesized Ag-NPs at 2.5, 5, 10, and 15 mg L^{-1}.

Table 1. Effects of *Aloe vera*-synthesized Ag nanoparticles (Ag-NPs) on chlorophyll (*a* and *b*), total phenols, total soluble sugar, proline, and total crude protein of *Cucurbita pepo.* Values are presented as the mean ± SD. Different letters indicate significant differences between means ($LSD_{0.01}$). T1: Control (sterilized soil, no inoculation); T2: pathogen (*Fusarium oxysporum* inoculated soil); T3: foliar spray of *A. vera*-synthesized Ag-NPs at 2.5, 5, 10, 15 mg L^{-1} (sterilized soil, applied days 5 and 20); T4: seeds planted in soil pre-treated with *A. vera*-synthesized Ag-NPs at 2.5, 5, 10, and 15 mg L^{-1}; T5: combined treatment with planted seeds in *Fusarium*-inoculated soil and seedlings received foliar sprays of *A. vera*-synthesized Ag-NPs at 2.5, 5, 10, and 15 mg L^{-1}.

Treatments		Chlorophyll *a*	Chlorophyll *b*	Total phenols	Total soluble sugar	Proline content	Total protein content
	mg L^{-1}	mg g^{-1} FW	mg g^{-1} FW	µg g^{-1} FW	mg g^{-1}	µmol g^{-1}	mg g^{-1}
T1: Control		1.5 ± 0.035^{d}	1.2 ± 0.033^{de}	2.04 ± 0.053^{d}	4.00 ± 0.101^{g}	22.16 ± 0.582^{g}	19.6 ± 0.505^{h}
T2: Pathogen		0.8 ± 0.021^{h}	0.5 ± 0.013^{h}	3.56 ± 0.093^{c}	5.75 ± 0.159^{b}	24.30 ± 0.619^{c}	20.3 ± 0.569^{g}
T3: Ag-NPs spray	2.5	1.5 ± 0.035^{cd}	1.3 ± 0.033^{d}	2.33 ± 0.0531^{c}	4.20 ± 0.119^{f}	22.40 ± 0.582^{f}	20.8 ± 0.489^{f}
	5	1.7 ± 0.042^{c}	1.5 ± 0.035^{cd}	2.58 ± 0.0542^{f}	4.61 ± 0.124^{de}	23.50 ± 0.619^{e}	21.5 ± 0.569^{de}
	10	1.9 ± 0.053^{ab}	1.6 ± 0.042^{c}	2.85 ± 0.093^{e}	4.73 ± 0.129^{d}	24.60 ± 0.635^{c}	21.9 ± 0.569^{d}
	15	2.3 ± 0.053^{a}	1.8 ± 0.053^{a}	3.00 ± 0.093^{d}	4.84 ± 0.132^{c}	25.21 ± 0.672^{b}	22.3 ± 0.603^{c}
T4: Ag-NPs soil pre-treated	2.5	1.4 ± 0.035^{de}	1.2 ± 0.029^{de}	2.26 ± 0.0531^{c}	$4.00 \pm 0.0.101^{g}$	22.20 ± 0.582^{f}	20.2 ± 0.487^{f}
	5	1.6 ± 0.042^{ed}	1.3 ± 0.029^{d}	2.54 ± 0.0531^{f}	4.50 ± 0.119^{e}	23.20 ± 0.608^{e}	21.1 ± 0.555^{e}
	10	1.8 ± 0.053^{b}	1.5 ± 0.035^{cd}	2.81 ± 0.093^{ef}	4.62 ± 0.124^{de}	24.10 ± 0.635^{d}	21.6 ± 0.569^{de}
	15	2.2 ± 0.053^{a}	1.6 ± 0.042^{b}	2.91 ± 0.093^{de}	4.82 ± 0.132^{c}	25.00 ± 0.672^{bc}	22.1 ± 0.569^{c}
T5: Ag-NPs spray + pathogen	2.5	0.9 ± 0.029^{g}	0.6 ± 0.0164^{g}	2.50 ± 0.053^{fg}	4.30 ± 0.101^{ef}	22.30 ± 0.603^{f}	21.3 ± 0.569^{e}
	5	1.2 ± 0.033^{f}	0.8 ± 0.021^{f}	3.64 ± 0.093^{b}	5.60 ± 0.148^{bc}	23.70 ± 0.619^{de}	22.5 ± 0.603^{bc}
	10	1.4 ± 0.035^{de}	0.8 ± 0.021^{f}	4.82 ± 0.123^{ab}	5.90 ± 0.148^{ab}	25.10 ± 0.664^{bc}	22.9 ± 0.603^{b}
	15	1.7 ± 0.042^{c}	1.0 ± 0.0288^{e}	4.98 ± 0.123^{a}	6.50 ± 0.175^{a}	26.70 ± 0.712^{a}	23.3 ± 0.619^{a}

Table 2. Effects of *Aloe vera*-synthesized Ag nanoparticles (Ag-NPs) on the elemental composition (Ca^{+2}, Mg^{+2}, Na^{+}, K^{+}) (%) of *Cucurbita pepo.* Values are presented as the mean ± SD. Different letters indicate significant differences between means ($LSD_{0.01}$). T1: Control (sterilized soil, no inoculation); T2: pathogen (*Fusarium oxysporum* inoculated soil); T3: foliar spray of *A. vera*-synthesized Ag-NPs at 2.5, 5, 10, 15 mg L^{-1} (sterilized soil, applied days 5 and 20); T4: seeds planted in soil pre-treated with *A. vera*-synthesized Ag-NPs at 2.5, 5, 10, and 15 mg L^{-1}; T5: combined treatment with planted seeds in *Fusarium*-inoculated soil and seedlings received foliar sprays of *A. vera*-synthesized Ag-NPs at 2.5, 5, 10, and 15 mg L^{-1}.

Treatments	mg L^{-1}	Calcium (Ca^{+2})	Magnesium (Mg^{+2})	Sodium (Na^{+})	Potassium (K^{+})
T1: Control		1.13 ± 0.033^{f}	0.30 ± 0.009^{g}	1.10 ± 0.033^{f}	1.02 ± 0.0288^{f}
T2: Pathogen		0.70 ± 0.0185^{i}	0.10 ± 0.0029^{k}	0.20 ± 0.005^{i}	0.70 ± 0.0185^{d}
T3: Ag-NPs spray	2.5	2.77 ± 0.079^{de}	0.54 ± 0.01^{d}	1.30 ± 0.033^{e}	1.42 ± 0.033^{de}
	5	2.91 ± 0.079^{cd}	0.57 ± 0.0156^{cd}	1.45 ± 0.033^{c}	1.90 ± 0.053^{cd}
	10	3.31 ± 0.093^{b}	0.59 ± 0.0156^{b}	1.49 ± 0.053^{b}	2.03 ± 0.053^{b}
	15	3.58 ± 0.101^{a}	0.63 ± 0.0164^{a}	1.55 ± 0.053^{a}	2.52 ± 0.093^{a}
T4: Ag-NPs soil pre-treated	2.5	2.42 ± 0.053^{e}	0.48 ± 0.0127^{fg}	1.20 ± 0.033^{ef}	1.34 ± 0.033^{e}
	5	2.80 ± 0.079^{d}	0.51 ± 0.0137^{f}	1.40 ± 0.033^{de}	1.70 ± 0.033^{d}
	10	3.10 ± 0.079^{c}	0.52 ± 0.0137^{e}	1.45 ± 0.053^{bc}	1.98 ± 0.053^{c}
	15	3.51 ± 0.093^{ab}	0.59 ± 0.0156^{b}	1.50 ± 0.053^{ab}	2.00 ± 0.053^{b}
T5: Ag-NPs spray + pathogen	2.5	0.75 ± 0.021^{h}	0.12 ± 0.0031^{k}	0.45 ± 0.012^{h}	0.75 ± 0.02^{i}
	5	0.95 ± 0.026^{g}	0.19 ± 0.005^{j}	0.45 ± 0.012^{h}	0.90 ± 0.024^{h}
	10	0.95 ± 0.026^{g}	0.22 ± 0.0058^{i}	0.55 ± 0.0145^{g}	0.95 ± 0.025^{g}
	15	1.00 ± 0.0288^{fg}	0.25 ± 0.0069^{h}	0.56 ± 0.0156^{fg}	1.00 ± 0.0288^{f}

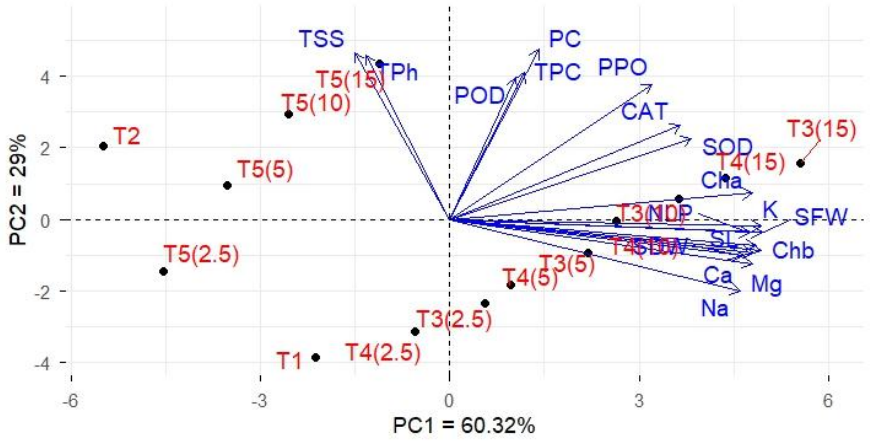

Figure 5. Principal component biplot of growth, biochemical, and mineral traits of *Cucurbita pepo* as affected by *Aloe vera*-synthesized Ag nanoparticles (Ag-NPs) treatments under *Fusarium oxysporum* stress. T1: Control (sterilized soil, no inoculation); T2: pathogen (*F. oxysporum* inoculated soil); T3: foliar spray of *Aloe vera*-synthesized Ag-NPs at 2.5, 5, 10, 15 mg L^{-1} (sterilized soil, applied days 5 and 20); T4: seeds planted in soil pre-treated with *A. vera*-synthesized Ag-NPs at 2.5, 5, 10, and 15 mg L^{-1}; T5: combined treatment with planted seeds in *Fusarium*-inoculated soil and seedlings received foliar sprays of *A. vera*-synthesized Ag-NPs at 2.5, 5, 10, and 15 mg L^{-1}; Cha: chlorophyll *a*; Chb: Chlorophyll *b*; NLP: number of leaves per plant; SL: shoot length; SFW: shoot fresh weight; SDW: shoot dry weight; SOD: superoxide dismutase; PPO: polyphenol oxidase; CAT: catalase; POD: peroxidase; TPh: total phenolic content; TSS: total soluble sugars; PC: proline content; TPC: total protein content.

Relationships among treatments and studied traits

The principal component analysis (PCA) grouped the treatments into distinct clusters (Figure 5). The PCA explained 60.32% of the total variability on PC1 and 29% on PC2. Along PC1, the Ag-NPs treatments T3(15), T4(15), T3(10) and T4(10) were separated on the positive side. These treatments were associated with improved growth-related and nutritional traits. Whereas the control (T1) and pathogen-only treatment (T2) were located on the negative side of PC1. These treatments were associated with reduced growth and mineral contents. Along PC2, the combined pathogen plus Ag-NPs treatments (T5), particularly T5(15) and T5(10), showed high positive scores. These treatments were closely associated with higher total soluble sugars (TSS) and total phenolic content (TPh). The antioxidant enzymes (CAT, SOD, PPO, POD), total protein content (TPC), and proline content (PC) were positively associated with T3(15). The hierarchical clustering heatmap further presented the contrasting responses of *C. pepo* to *A. vera*-synthesized Ag-NPs under *F. oxysporum* stress (Figure 6). Infected plants treated with Ag-NPs at low dose T5(2.5) were grouped with the pathogen-only treatment T2. These treatments were characterized by low values of chlorophyll *a* and *b*, shoot length and biomass, and macroelements. By contrast, higher Ag-NP doses, particularly T3(10-15) and T4(10-15), clustered together. These treatments were associated with elevated growth traits (NLP, SL, SFW, SDW) and increased K, Ca and Mg contents, and antioxidant enzyme activities.

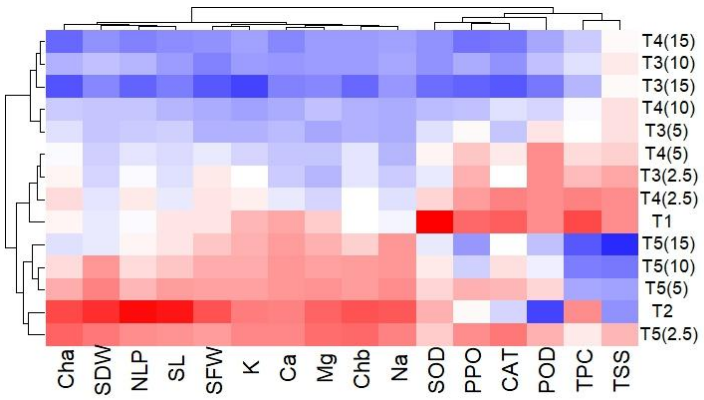

Figure 6. Hierarchical clustering heatmap of growth, biochemical, and mineral parameters of *Cucurbita pepo* under *Fusarium oxysporum* infection as affected by *Aloe vera*-synthesized Ag nanoparticle (Ag-NPs) treatments. T1: Control (sterilized soil, no inoculation); T2: pathogen (*F. oxysporum* inoculated soil); T3: foliar spray of *A. vera*-synthesized Ag-NPs at 2.5, 5, 10, 15 mg L^{-1} (sterilized soil, applied days 5 and 20); T4: seeds planted in soil pre-treated with *A. vera*-synthesized Ag-NPs at 2.5, 5, 10, and 15 mg L^{-1}; T5: combined treatment with planted seeds in *Fusarium*-inoculated soil and seedlings received foliar sprays of *A. vera*-synthesized Ag-NPs at 2.5, 5, 10, and 15 mg L^{-1}; Cha: chlorophyll *a*; Chb: chlorophyll *b*; NLP: number of leaves per plant; SL: shoot length; SFW: shoot fresh weight; SDW: shoot dry weight; SOD: superoxide dismutase; PPO: polyphenol oxidase; CAT: catalase; POD: peroxidase; TPh: total phenolic content; TSS: total soluble sugars; PC: proline content; TPC: total protein content.

DISCUSSION

Fusarium wilt caused by *Fusarium oxysporum* poses a major threat to *Cucurbita pepo* production worldwide. This requires sustainable alternatives to enhance resistance and reduce environmental harm. This study evaluated the antifungal efficacy of Ag-nanoparticles (Ag-NPs) on *Fusarium oxysporum* in vitro inhibition and in vivo greenhouse trials. *Aloe vera* leaf extract effectively assisted as a reducing and capping agent in Ag-NPs biosynthesis. This was confirmed by phytochemical screening, revealing flavonoids, glycosides, saponins, steroids, and alkaloids. This rich profile reinforces the green synthesis superiority over chemical methods (Garg et al., 2019). Multiple techniques validated Ag-NP formation by color shift (greenish-yellow to brown), surface plasmon resonance (SPR) peak at 413 nm (UV-Vis), and Fourier-transform infrared spectroscopy (FTIR) bands (Pasieczna-Patkowska et al., 2025).

The results of in vitro trial demonstrated strong antifungal activity of *A. vera*-synthesized Ag-NPs against *F. oxysporum*. All tested concentrations inhibited fungal growth. This confirms the efficacy of the Ag-NPs as a fungicidal agent. This inhibition was dose-dependent, which is consistent with the principles of toxicology and pharmacology. The increased concentration of Ag-NPs from 2.5 to 15 mg L^{-1} caused considerable increase in the inhibition zone. This indicates positive relationship between the concentration of the nanoparticle and antifungal effect (Hashem et al., 2022).

The results of the greenhouse trials displayed significant negative effects of *F. oxysporum* on *C. pepo*. All measured growth parameters in the inoculated control (T2) were significantly reduced compared to the uninoculated control (T1). All Ag-NPs treatments considerably improved plant growth parameters compared to the infected control (T2). All applications of foliar spray and soil pre-treated displayed significant improvement in plant growth parameters. This suggests dual mode of action for the nanoparticles using foliar spray or soil pre-treated (Arsène et al., 2023). The foliar spray in particular concentration of 15 mg L^{-1} displayed the highest growth parameters. Besides, in the presence of the pathogen, the Ag-NPs treatments enhanced plant growth compared to the inoculated control (T2). The combined application of 15 mg L^{-1} Ag-NPs and the pathogen led to a significant increase in plant growth. This demonstrates a powerful protective effect of Ag-NPs at 15 mg L^{-1}. This suggests that the nanoparticles suppressed the pathogen population. In this context, Macías Sánchez et al.

(2023) reported that Ag-NPs strongly inhibited *F. oxysporum*. Moreover, Khan et al. (2023) elucidated that Ag-NPs can enhance seed germination, plant growth, and photosynthetic efficiency. It can act as effective nano-fertilizers and nano-pesticides when applied at appropriate concentrations. This emphasizes that Ag-NPs provide antifungal protection to contribute to crop protection.

The effect of Ag-NPs on biochemical parameters of *C. pepo* under *F. oxysporum* infection was assessed. The Ag-NPs spray in infected plants (T5) showed significant improvement in chlorophylls, phenols, and soluble sugars. This indicates that the Ag-NPs enhanced the defense systems of *C. pepo* under infection conditions. Besides, higher levels of chlorophyll *a* and *b* indicate improved photosynthetic efficiency. In this context, Cheaib and Killiny (2025) elucidated that pathogen infection reduces plant photosynthesis through two main scenarios. The first involves pathogens attacking green aerial tissues. This causes a decrease in the overall photosynthetic area. The second scenario involves chlorosis caused by a reduction in chlorophyll content per chloroplast. Even in the absence of the pathogen, the Ag-NPs-treated groups (T3 and T4) showed an increase in these beneficial compounds. This indicates that the nanoparticles passively fighting the pathogen and also acting as biostimulants to promote plant vigor (Magnabosco et al., 2023). The elemental analysis further confirmed the positive impact of nanoparticles. The fungal infection significantly reduced nutrient uptake. However, Ag-NP treatments enhanced the levels of minerals Ca^{2+}, Mg^{2+}, and K^{+}. This effect improves the plant health and nutrient absorption (Alfosea-Simón et al., 2025). The enzyme analysis showed that *F. oxysporum* infection significantly increased the activity of defense enzymes (catalase, superoxide dismutase, polyphenol oxidase, and peroxidase). However, treatment with Ag-NPs had a beneficial effect. Ag-NPs boosted enzyme levels in a dose-dependent manner and enhanced the plant defenses (Sharma et al., 2025). The Ag-NPs applications under infection stress reduced the stress-induced enzyme activity. This indicates that the nanoparticles effectively mitigated the source of stress.

Multivariate analysis is important to explore multiple traits in experimental treatments (Rehman et al., 2019). These tools are valuable to summarize complex growth, biochemical, and mineral performance to present the effective Ag-NP treatments and their effects on *Fusarium* stress. The PCA biplot provided separation of T3 (10-15) on the positive side of PC1. These treatments displayed a positive association with shoot biomass, chlorophylls, and essential mineral elements. This supports that the foliar application of higher Ag-NP doses primarily acts as a growth-promoting and nutrition-enhancing strategy in non-infected plants. In contrast, T1 and T2 were located at the negative side of PC1, away from the most beneficial traits. This emphasizes that the absence of nanoparticles and the presence of the pathogen alone are associated with poor growth and nutrient status. Moreover, the heatmap grouped high-dose foliar and soil-treated treatments T3(10-15) and T4(10-15) with elevated leaf number, shoot length, biomass, and macronutrient contents. This indicates that, in the absence of disease pressure, Ag-NPs act as biostimulants. Conversely, infected plants treated with Ag-NPs at low dose T5 (2.5) and the infected control (T2) associated with poor growth. These treatments recorded low chlorophylls and minerals, and antioxidant profiles. This indicates that suboptimal Ag-NP doses are insufficient to respond to *Fusarium* stress. The PCA and heatmap reinforce that Ag-NPs stimulate healthy plants and activate biochemical and antioxidant defenses in infected plants. This indicates their potential use in disease management.

CONCLUSIONS

This study demonstrates that *Aloe vera*-mediated Ag nanoparticles (Ag-NPs) are an effective strategy for managing *Fusarium* wilt in *Cucurbita pepo*. Biogenic Ag-NPs strongly suppressed *F. oxysporum* growth in vitro. Moreover, it alleviated disease symptoms and growth suppression in vivo. Under greenhouse conditions, Ag-NP treatments significantly improved shoot length, leaf number, and shoot biomass in healthy and infected plants. Moreover, Ag-NP significantly enhanced chlorophylls, total phenols, soluble sugars, proteins, and mineral nutrients. In addition, Ag-NPs modulated the activities of catalase, superoxide dismutase, polyphenol oxidase, and peroxidase in non-infected and infected plants. Multivariate analyses confirmed that high Ag-NP doses are associated with superior growth, nutritional status, and reinforced biochemical defenses. *Aloe vera*-synthesized Ag-NPs act as strong antifungal agents and plant biostimulants. It enhanced resistance to *F. oxysporum* and the physiological performance of *C. pepo*. These findings indicate green-synthesized Ag-NPs as a promising, eco-friendly component of integrated disease management programs for cucurbits.

Author contribution

Conceptualization: E.Se., E.Sa., Y.S., M.I.A., E.F., A.A.S.A., H.Al., H.Ab. Methodology: E.Se., E.Sa., Y.S., M.I.A., E.F., A.A.S.A., H.Al., H.Ab. Software: E.Se., E.Sa., Y.S., M.I.A., E.F., A.A.S.A., H.Al., H.Ab. Validation: E.Se., E.Sa., Y.S., M.I.A., E.F., A.A.S.A., H.Al., H.Ab. Formal analysis: E.Se., E.Sa., Y.S., M.I.A., E.F., A.A.S.A., H.Al., H.Ab. Investigation: E.Se., E.Sa., Y.S., M.I.A., E.F., A.A.S.A., H.Al., H.Ab. Resources: E.Se., E.Sa., Y.S., M.I.A., E.F., A.A.S.A., H.Al., H.Ab. Data curation, E.Se., E.Sa., Y.S., M.I.A., E.F., A.A.S.A., H.Al., H.Ab. Writing original draft preparation: E.Se., E.Sa., Y.S., M.I.A., E.F., A.A.S.A., H.Al., H.Ab. Supervision E.S., E.S., Y.S., M.I.A., E.F., A.A.S.A., H.A., H.A. Funding acquisition E.Se., E.Sa., Y.S., M.I.A., E.F., A.A.S.A., H.Al., H.Ab. All co-authors reviewed the final version and approved the manuscript before submission.

Acknowledgments

The authors extend their appreciation for the Princess Nourah bint Abdulrahman University Researchers Supporting Project number (PNURSP2026R84), Princess Nourah bint Abdulrahman University, Riyadh, Saudi Arabia.

References

Abdalla, H., Adarosy, M.H., Hegazy, H.S., Abdelhameed, R.E. 2022. Potential of green synthesized titanium dioxide nanoparticles for enhancing seedling emergence, vigor and tolerance indices and DPPH free radical scavenging in two varieties of soybean under salinity stress. BMC Plant Biology 22(1):560. doi:10.1186/s12870-022-03945-7.

Akpinar, I., Unal, M., Sar, T. 2021. Potential antifungal effects of silver nanoparticles (AgNPs) of different sizes against phytopathogenic *Fusarium oxysporum* f. sp. *radicis-lycopersici* (FORL) strains. Applied Sciences 3(4):506. doi:10.1007/s42452-021-04524-5.

Alahmari, A.S., Magdy, M., El-Mansy, A.B., Awad, N.S., Eldenary, M.E., Alshamrani, R., et al. 2025. Evaluation of nanoparticle biostimulants in alleviating salinity-induced stress: A study on morphological and molecular responses in potato cultivars. Chilean Journal of Agricultural Research 85:414-423. doi:10.4067/S0718-58392025000300414.

Alfosea-Simón, F.J., Burgos, L., Alburquerque, N. 2025. Silver nanoparticles help plants grow, alleviate stresses, and fight against pathogens. Plants 14(3):428. doi:10.3390/plants14030428.

Alowaiesh, B.F., Awad, N.S., Eldenary, M.E., Abd El Moneim, D. 2024. Enhancement of drought tolerance in potato employing nanoparticles of different biostimulants. Chilean Journal of Agricultural Research 84:246-259. doi:10.4067/S0718-58392024000200246.

Alwan, A.I.J., Nulit, R., Go, R., Hadwan, M.H. 2026. Nano-priming with calcium silicate nanoparticles (CaSiO3NPs) promotes germination, seedling growth, and antioxidant enzyme activity in Iraqi rice genotypes under drought stress. Chilean Journal of Agricultural Research 86:129-139. doi:10.4067/S0718-58392026000100129.

Arsène, M.M.J., Viktorovna, P.I., Alla, M., Mariya, M., Nikolaevitch, S.A., Davares, A.K.L., et al. 2023. Antifungal activity of silver nanoparticles prepared using *Aloe vera* extract against *Candida albicans*. Veterinary World 16(1):18-26. doi:10.14202/vetworld.2023.18-26.

Bates, L.S., Waldren, R.P., Teare, I.D. 1973. Rapid determination of free proline for water-stress studies. Plant and Soil 39(1):205-207. doi:10.1007/BF00018060.

Bergmeyer, H.-U. 1965. Methods of enzymatic analysis. 2nd ed. Verlag Chemie, Wiley, New York, USA.

Burange, P.J., Tawar, M.G., Bairagi, R.A., Malviya, V.R., Sahu, V.K., Shewatkar, S.N., et al. 2021. Synthesis of silver nanoparticles by using *Aloe vera* and *Thuja orientalis* leaves extract and their biological activity: A comprehensive review. Bulletin of the National Research Centre 45(1):181. doi:10.1186/s42269-021-00639-2.

Cheaib, A., Killiny, N. 2025. Photosynthesis responses to the infection with plant pathogens. Molecular Plant-Microbe Interactions 38(1):9-29. doi:10.1094/mpmi-05-24-0052-cr.

Choi, I.Y ,.Kim, J.H., Lee, W.H., Park, J.H., Shin, H.D. 2015. First report on *Fusarium* wilt of zucchini caused by *Fusarium oxysporum*, in Korea. Mycobiology 43(2):174-178. doi:10.5941/myco.2015.43.2.174.

Dhindsa, R.S., Plumb-Dhindsa, P., Thorpe, T.A. 1981. Leaf senescence: Correlated with increased levels of membrane permeability and lipid peroxidation, and decreased levels of superoxide dismutase and catalase. Journal of Experimental Botany 32(1):93-101. doi:10.1093/jxb/32.1.93.

Garg, S.K., Shukla, A., Choudhury, S. 2019. Polyphenols and flavonoids. p. 187-204. In Gupta, R.C., Srivastava, A., Lall, R. (eds.) Nutraceuticals in veterinary medicine. Springer International Publishing, Cham, Switzerland. doi:10.1007/978-3-030-04624-8.

Gilardi, G., Pugliese, M., Garibaldi, A., Gullino, M.L. 2024. Emerging vegetable crop diseases and their management options. CABI Reviews 19:1. doi:10.1079/cabireviews.2024.0007.

Gonzalez-Jimenez, I., Perlin, D.S., Shor, E. 2023. Reactive oxidant species induced by antifungal drugs: Identity, origins, functions, and connection to stress-induced cell death. Frontiers in Cellular and Infection Microbiology 13:1276406. doi:10.3389/fcimb.2023.1276406.

Grumet, R., McCreight, J.D., McGregor, C., Weng, Y., Mazourek, M., Reitsma, K., et al. 2021. Genetic resources and vulnerabilities of major cucurbit crops. Genes 12(8):1222. doi:10.3390/genes12081222.

Hashem, A.H., Saied, E., Amin, B.H., Alotibi, F.O., Al-Askar, A.A., Arishi, A.A., et al. 2022. Antifungal activity of biosynthesized silver nanoparticles (AgNPs) against *Aspergilli* causing Aspergillosis: Ultrastructure study. Journal of Functional Biomaterials 13(4):242. doi:10.3390/jfb13040242.

Iqbal, E., Salim, K.A., Lim, L.B. 2015. Phytochemical screening, total phenolics and antioxidant activities of bark and leaf extracts of *Goniothalamus velutinus* (Airy Shaw) from Brunei Darussalam. Journal of King Saud University-Science 27(3):224-232. doi:10.1016/j.jksus.2015.02.003.

Jindal, K.K., Singh, R.N. 1975. Phenolic content in male and female *Carica papaya*: A possible physiological marker for sex identification of vegetative seedlings. Physiologia Plantarum 33(1):104-107. doi:10.1111/j.1399-3054.1975.tb03774.x.

Joudeh, N., Linke, D. 2022. Nanoparticle classification, physicochemical properties, characterization, and applications: A comprehensive review for biologists. Journal of Nanobiotechnology 20(1):262. doi:10.1186s12951-022-01477-8.

Khan, S., Zahoor, M., Sher Khan, R., Ikram, M., Islam, N.U. 2023. The impact of silver nanoparticles on the growth of plants: The agriculture applications. Heliyon 9(6):16928. doi:10.1016/j.heliyon.2023.e16928.

Macías Sánchez, K.L., González Martínez, H.D., Carrera Cerritos, R., Martínez Espinosa, J.C. 2023. In Vitro evaluation of the antifungal effect of AgNPs on *Fusarium oxysporum* f. sp. *lycopersici*. Nanomaterials 13(7):1274. doi:10.3390/nano13071274.

Magalhães, I.C., Souza, G.T., Souza, M.R., Torquato, I.H., Santos, A.M., Castro, C.C. 2025. Global review of zucchini (*Cucurbita pepo*) pollination: Research approaches, distribution of pollinators and knowledge gaps. Revista Ciência Agronômica 56:e202392319. doi:10.5935/1806-6690.20250031.

Magnabosco, P., Masi, A., Shukla, R., Bansal, V., Carletti, P. 2023. Advancing the impact of plant biostimulants to sustainable agriculture through nanotechnologies. Chemical and Biological Technologies in Agriculture 10(1):117. doi:10.1186/s40538-023-00491-8.

Metzner, H., Rau, H., Senger, H. 1965. Untersuchungen zur Synchronisierbarkeit einzelner Pigmentmangel-Mutanten von Chlorella. Planta 65(2):186-194. doi:10.1007/BF00384998.

Naga Raju, G.J., Sarita, P., Ramana Murty, G.A.V., Ravi Kumar, M., Seetharami Reddy, B., John Charles, M., et al. 2006. Estimation of trace elements in some anti-diabetic medicinal plants using PIXE technique. Applied Radiation and Isotopes 64(8):893-900. doi:10.1016/j.apradiso.2006.02.085.

Ong, J.X., Abd Murad, N.B., Rasli, S.R.A.M., Zakaria, M.R.S., Selvamani, S., El-Enshasy, H.A., et al. 2025. Black soldier fly frass and its derivatives as biofungicide to control Fusarium wilt in bananas. Chilean Journal of Agricultural Research 85:469-479. doi:10.4067/S0718-58392025000300469.

Pasieczna-Patkowska, S., Cichy, M., Flieger, J. 2025. Application of Fourier transform infrared (FTIR) spectroscopy in characterization of green synthesized nanoparticles. Molecules 30(3):684. doi:10.3390/molecules30030684.

Prud'homme, M.P., Gonzalez, B., Billard, J.P., Boucaud, J. 1992. Carbohydrate content, fructan and sucrose enzyme activities in roots, stubble and leaves of ryegrass (*Lolium perenne* L.) as affected by source/sink modification after cutting. Journal of Plant Physiology 140(3):282-291. doi:10.1016/S0176-1617(11)81080-1.

Qureshi, A.K., Farooq, U., Shakeel, Q., Ali, S., Ashiq, S., Shahzad, S., et al. 2023. The green synthesis of silver nanoparticles from *Avena fatua* extract: Antifungal activity against *Fusarium oxysporum* f.sp. *lycopersici*. Pathogens 12(10):1247. doi:10.3390/pathogens12101247.

Rehman, F., Saeed, A., Yaseen, M., Shakeel ,A., Ziaf, K., Munir, H., et al. 2019. Genetic evaluation and characterization using cluster heat map to assess NaCl tolerance in tomato germplasm at the seedling stage. Chilean Journal of Agricultural Research 79:56-65. doi:10.4067/S0718-58392019000100056.

Sharma, M.M.M., Kapoor, D., Loyal, A., Kumar, R., Sharma, P., Husen, A. 2025. Plant response to silver nanoparticles in terms of growth, development, production, and protection: An overview. p. 1-22. In Husen, A. (ed.) Plant response to silver nanoparticles: Plant growth, development, production, and protection. Springer Nature, Singapore**.** doi:10.1007/978-981-97-7352-7_1.

Silva, T.E., Detmann, E., Franco, M.O., Palma, M.N., Rocha, G.C. 2016. Evaluation of digestion procedures in Kjeldahl method to quantify total nitrogen in analyses applied to animal nutrition. Acta Scientiarum. Animal Sciences 38(1):45-51. doi:10.4025/actascianimsci.v38i1.29171.

Soliva, R.C., Elez, P., Sebastián, M., Martín, O. 2000. Evaluation of browning effect on avocado purée preserved by combined methods. Innovative Food Science & Emerging Technologies 1(4):261-268. doi:10.1016/S1466-8564(00)00033-3.

Usman, M., Atiq, M., Rajput, N.A., Sahi, S.T., Shad, M., Lili, N., et al. 2024. Efficacy of green synthesized silver based nanomaterials against early blight of tomato caused by *Alternaria solani*. Journal of Crop Health 76(1):105-115. doi:10.1007/s10343-023-00957-7.

Wu, S., Yue, Y., Tian, H., Li, Z., Li, X., He, W., et al. 2013. Carthamus red from *Carthamus tinctorius* L. exerts antioxidant and hepatoprotective effect against CCl_4-induced liver damage in rats via the Nrf2 pathway. Journal of Ethnopharmacology 148(2):570-578. doi:10.1016/j.jep.2013.04.054.